# Effect of Interfacial Attraction on Intercalation in Polymer/Clay Nanocomposites

**Sang-Soo Lee,[1] Myung Hyun Hur,[2] Hoichang Yang,[3] Soonho Lim,[1] Junkyung Kim[1]**

[1]*Polymer Hybrid Research Center, Korea Institute of Science and Technology, Seoul 136-791, Korea*
[2]*Department of Chemical Engineering, Kwangwoon University, Seoul 139-050, Korea*
[3]*Rensselaer Nanotechnology Center, Rensselaer Polytechnic Institute, Troy, New York 12180*

Received 17 May 2004; accepted 25 April 2005
DOI 10.1002/app.23027
Published online 2 June 2006 in Wiley InterScience (www.interscience.wiley.com).

**ABSTRACT:** In order to examine the adhesive behavior of a polar polymer between hydrophilic clay layers, the so-called glue effect, a clay intercalation by an ethylene–vinyl alcohol (EVOH) copolymer, which was capable of strong hydrogen bonding with the silicate surface of clay, was prepared by the melt intercalation technique and compared with a clay nanocomposite containing styrene–acrylonitrile (SAN) copolymer of less polar interaction energy in terms of the morphology and mechanical properties. Although initial penetration of the guest polymer into the gallery of the host clay occurred more rapidly for EVOH because of its strong hydrophilic nature, the dissociation of clay nanoplatelets was better developed for SAN with less polar interaction with clay, well evidencing the fact that the glue effect effectively affects the intercalation behavior of polymer/clay nanocomposites. However, the mechanical properties of the EVOH/clay nanocomposite were superior to those of SAN/clay nanocomposites. Although dissociation of respective silicate layers was poor for EVOH/clay nanocomposites, strong attractive energy stabilizes the interface between inorganic nanoparticles and the polymer matrix much more effectively, resulting in higher mechanical properties. © 2006 Wiley Periodicals, Inc. J Appl Polym Sci 101: 2749–2753, 2006

**Key words:** nanocomposites; hydrogen bonding; ethylene–vinyl alcohol; styrene–acrylonitrile; clay

## INTRODUCTION

To date, numerous studies concerning fabrication of polymer/clay nanocomposites have reported that polymers with polar groups should be used to obtain a highly intercalated structure or exfoliation state.[1–16] When a polymer with polar functional groups was introduced into the clay gallery, some of the recent theoretical and experimental research results demonstrated that the adhesive role of a polar polymer between hydrophilic clay layers, the so-called glue effect, tends to strongly prohibit complete dissociation of the layered structure of clay, resulting in only an ordered intercalated state.[17–22]

At this point we need to elucidate the role of the interaction energy at the interface between a clay and polymer intercalant, of which the molecular architecture is of prominent importance for control of the intercalation and the corresponding material properties of the resulting nanocomposites. It has been speculated that the degree of intercalation is determined as a function of the cation exchange capacity of clay and the molecular structures of the intercalant molecules, such as the conformation geometry of a hydrocarbon tail, the cross-sectional dimension, and the functional group of the intercalant molecules. Among various factors influencing intercalation, we focus on the effect of specific interactions such as hydrogen bonding, because clay has a strong hydrophilic nature through its large population of polar functional groups on the surface, and entropic gain as the driving force for the penetration of a guest polymer into the gallery of the host clay; although not ignorable, it has been estimated to be not great.

Our previous works[20–22] have demonstrated that the change of the polar interaction energy affects the initial intercalation rate of a polymer and the final degree of intercalation when varying the acrylonitrile (AN) content of styrene–AN (SAN) copolymer in SAN/clay nanocomposites systems. However, the change in the interaction energy by varying the AN in SAN/clay systems has been found to be not great. Thus, more prominent evidence should be acquired for a better understanding of which and how intercalation of polymer/clay nanocomposites systems is governed. For this purpose, a clay intercalation by ethylene–vinyl alcohol (EVOH), which can have strong hydrogen bonding with the hydroxyl group on

*Correspondence to:* S.-S. Lee (s-slee@kist.re.kr).
Contract grant sponsors: Center for Advanced Materials Processing, 21st Century Frontier R&D Program, Ministry of Science and Technology, Korea; Korea Institute of Science and Technology; Ministry of Science and Technology, Korea; Pohang Acceleration Laboratory.

Journal of Applied Polymer Science, Vol. 101, 2749–2753 (2006)
© 2006 Wiley Periodicals, Inc.

**TABLE I**
**Characteristics of Polymers**

| Designation | Composition[a] | $M_w$[b] (g/mol) |
|---|---|---|
| SAN | AN content = 27 mol % | 120,000 |
| EVOH | VA content = 33 mol % | 150,000 |

[a] Obtained from $^1$H-NMR spectra.
[b] Measured on a GPC apparatus calibrated with polystyrene standards.

the silicate surface of clay, was conducted by the melt intercalation technique and compared with SAN/clay systems in terms of the morphology and mechanical properties.

## EXPERIMENTAL

### Materials

The characteristics of SAN (AN content = 27 mol %) and EVOH [vinyl alcohol (VA) content = 33 mol %] copolymers and various organoclays (organically modified montmorillonites) used in this study are listed in Tables I and II. For the removal of any impurities, the polymers were dissolved in respective solvents and precipitated with an excess amount of methanol. The crude precipitate was dried at 80°C for 24 h and ground into a fine powder.

Organoclays were received from Southern Clays as fine powders. They were washed with deionized water several times to remove excess ionic molecules and impurities. This was followed by centrifugation and vacuum drying at 100°C for 24 h. The chemical structure of the organic intercalant in the organoclays is as follows:

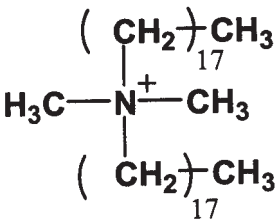

To obtain polymer/clay nanocomposites with the melt intercalation method, two kinds of melt intercalation methods were applied: melt intercalation by thermal diffusion (static melt intercalation) and melt intercalation by shear force (dynamic melt intercalation). Before intercalation, the purified polymer and various organoclays were dry mixed in a blender. After they were blended, the composition of mixing was determined to preserve the content of inorganic clay at 5 wt % in all cases. For static melt intercalation, a powdery mixture in an appropriate amount was placed on a molder and heated under a pressure of 5 atm with varying heating times at 150° for SAN and 190° for EVOH. In all cases, a vacuum system was attached to the compression molder to suppress oxidation and degradation of the polymer as much as possible. Afterward, the molder was quenched with liquid nitrogen to obtain a disk-shaped specimen (10 mm in diameter, 100 mm thick) for X-ray measurements and thermal analysis.

For dynamic melt intercalation, a twin-screw extruder with a 60-cm processing zone was used. Melt processing was repeated several times (usually 3 times) until no change in the X-ray diffraction (XRD) spectrum was obtained. After vacuum drying at 110°C for 24 h, the mixtures were compression molded into 10- and 1000-$\mu$m sheets for XRD and mechanical property measurements, respectively.

### Characterization

XRD spectra were collected on an XRD instrument (MacScience MXP18) in reflection mode. An X-ray generator was run at 18 kW and the target was a copper standard (I = 1.5405 Å). Scanning was performed for $2\theta$ 0.5–10° at a rate of 0.5°/min. The basal spacing of the layered silicates ($d_{001}$) was calculated with Bragg's law ($\lambda = 2d \sin \theta$), from the 001 peak position. Transmission electron microscopy (TEM) micrographs were taken of a microtomed section of the nanocomposites (about 100 nm thick) mounted in epoxy; a transmission electron microscope (JEM-2000FX, JEOL) with an acceleration voltage of 100 kV was used. The uniaxial tensile tests with dumbbell-shaped specimens were conducted on an Instron 4201 universal testing machine with a crosshead speed of 5 mm/min at ambient temperature.

## RESULTS AND DISCUSSION

Before the experimental examination of the interfacial affinity of EVOH and SAN to the silicate surface, Fedor's group contribution system[23] was adopted to calculate the solubility parameters of EVOH and SAN for the purpose of a comparison of the polarity. A solubility parameter of 25.4 $J^{1/2}/cm^{3/2}$ was found for EVOH containing 33 mol % VA, whereas it was 22.9

**TABLE II**
**Characteristics of Organoclays**

| Designation[a] | Interlayer distance, $d_{001}$ (Å) |
|---|---|
| 140C[a] | 34.7 |
| 125C | 23.6 |
| 95C | 18.9 |

[a] Designations such as 140C represents an organoclay derived from the pristine clay with a cation exchange capacity value of 140 meq/100 g clay.

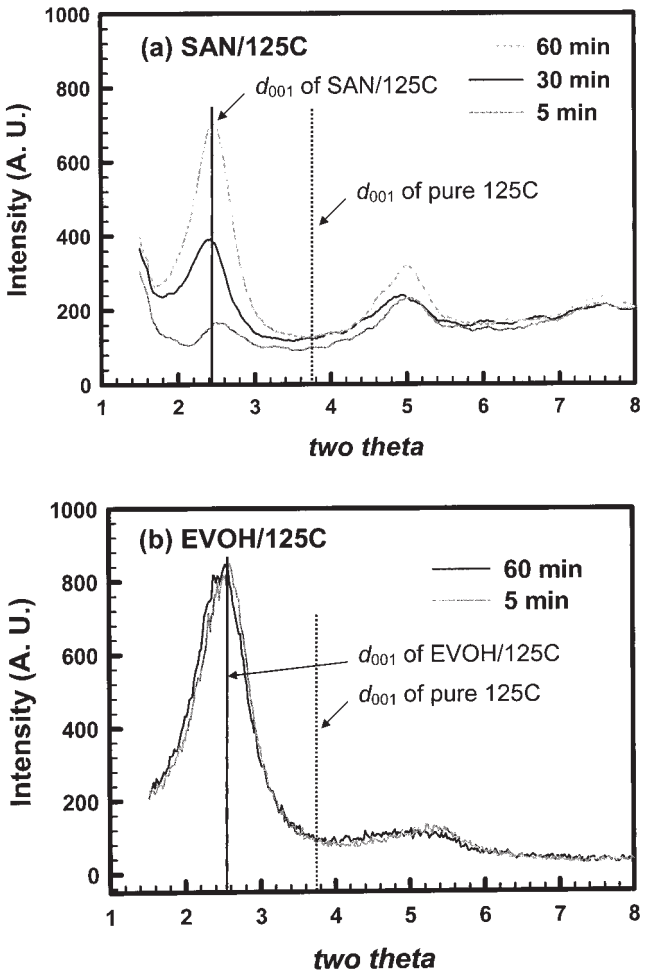


**Figure 1** XRD spectra of the intercalated clay nanoplatelets after static melt intercalation with varying heating times in (a) SAN/125C nanocomposites and (b) EVOH/125C nanocomposites. The $d_{001}$ peak positions of (—) nanocomposites and (- - -) pure 125C organoclay are shown.

$J^{1/2}/cm^{3/2}$ for SAN containing 27 mol % AN; this implies that, although the predicted value bears intrinsic inaccuracy to some extent, EVOH is more polar than SAN because of the large difference in the solubility parameter. Based on this calculation and the previous reports for the glue effect on intercalation behavior,[17–22] we expected that the degree of intercalation or disordering of silicate layers of organoclay for SAN would be more pronounced than that for EVOH because of the glue effect.

The nanocomposites of clay with EVOH as well as SAN prepared by static melt intercalation were examined by XRD measurements (Fig. 1). Figure 1 shows that, for all nanocomposites specimens, irrespective of the kind of organoclays, there is a shift of the (001) peak to lower $2\theta$, indicating the increase of the gallery height by polymer penetration for the EVOH/organoclay and SAN/organoclay nanocomposites. In addition, the degree of shift in the *d*-spacing seemed comparable for EVOH/organoclay and SAN/organoclay nanocomposites. In terms of the rate and degree of peak shift, however, there were noticeable differences between the two nanocomposite systems. For SAN/organoclay nanocomposites, the peak corresponding to the basal plane emerged progressively at around $2\theta$ 2.42° with the heating time, yielding a broad peak shape. In contrast, the peak of the basal plane was found at $2\theta$ 2.57° for EVOH/organoclay nanocomposites, which is slightly higher than that of SAN/organoclay nanocomposites, and a shift of the peak occurred nearly spontaneously. Under the assumption that the change in *d*-spacing ($\Delta d$-spacing) is directly proportional to the amount of polymer penetrating into the clay gallery, the acquired $\Delta d$-spacing was interpreted to represent that the amount of EVOH placed in the clay gallery was slightly lower than that of SAN, whereas the initial diffusion of polymer and the corresponding increase of the gallery height of the clay occurred more effectively by EVOH than by SAN. From these results, we concluded that a strong interaction energy between the polymer and clay does not guarantee a larger amount of polymer penetrating into the clay gallery and corresponding higher dissociation of clay platelets, whereas the initial diffusion rate of the guest polymeric molecules should be dependent on the polarity of the polymer. For clay–polymer mixtures, intercalation or exfoliation was determined by free-energy considerations through the modeling of a mixture of long-chain molecules and thin disks.[17–19] According to the modeling results, an exfoliated state can only occur for a positive Flory–Huggins interaction parameter between polymers and thin disks representing silicate layers, although the polymers and clay mixture will demix. In addition, an intercalated state is expected when an interaction parameter is negative from kinetic considerations. As the polymer diffuses through the energetically favorable gallery, it maximizes contact with the two confining silicate layers. A diffused polymer molecule glues the two adjacent surfaces together as it moves through the gallery, resulting in a kinetically trapped state. Consequently, although attractive energy between the polymer and clay is required for polymer diffusion into the gallery of silicate layers, increasing the attraction would only lead to an intercalated state, rather than an exfoliated one.

Figure 2 shows TEM micrographs of thin sections of SAN/125C and EVOH/125C nanocomposites prepared by dynamic melt intercalation, where the designation 125C represents an organoclay derived from the pristine clay with cation exchange capacity value of 125 meq/100 g clay. Contrary to the results found in the XRD spectra of nanocomposites by static melt intercalation, TEM bright field images reveal significant differences between SAN and EVOH; in EVOH/clay nanocomposites the silicate platelets are highly

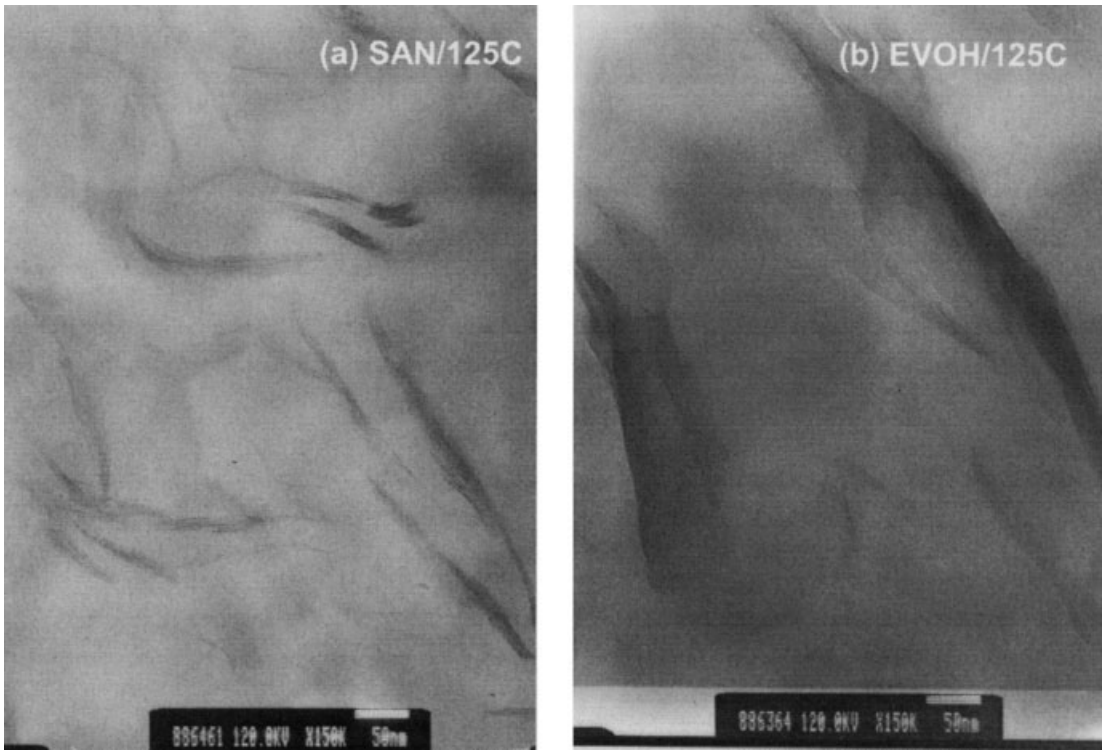


**Figure 2** TEM images of the intercalated clay nanoplatelets after dynamic melt intercalation in (a) SAN/clay nanocomposites and (b) EVOH/clay nanocomposites. A high association of clay nanoplatelets is evident for EVOH/clay nanocomposites.

associated to show a large domain of about 100-nm thickness, but in the SAN/clay nanocomposites the silicate platelets of 10 nm or less are associated to form a morphology like a thin thread. Because of the poor interfacial affinity for SAN/clay nanocomposites, the disintegration of the layered structure of clay was well developed when shear force was applied. Conversely, when EVOH/clay nanocomposites were prepared under strong shear force, the clay was able to associate more tightly because of the existence of EVOH between the silicate platelets acting as an adhesive, yielding less disintegration of the layered structure by shear force. This is well supported by the fact that the TEM image of EVOH/clay nanocomposites shows the boundary region between the clay and matrix is quite diffused and not discernable, so the interface is highly stabilized.

The mechanical properties were investigated to verify the dissociation of layered nanoplatelets of organoclays and their distribution on the polymer matrix in nanoscale, both of which were expected on the basis of XRD and TEM. Figure 3 depicts the results of the uniaxially tensioned specimens of nanocomposites as well as neat polymers. The figure shows that SAN/clay nanocomposites had poor mechanical properties; the tensile strengths of the nanocomposites dropped below that of neat SAN, whereas the modulus of the nanocomposites increased over that of neat SAN because of the presence of inorganic hard components. In contrast, EVOH/clay nanocomposites favored a dramatic increase of mechanical properties; there was a simultaneous enhancement of the tensile strength and modulus, which is supporting evidence of a highly stabilized interface for the EVOH/clay nanocomposites system.

Based on these findings, we concluded that the glue effect is important in determining the degree of intercalation, and the optimum value of interaction between the polymer and clay surface is of critical consideration in designing high performance clay nanocomposites with an intercalated structure.

## CONCLUSION

EVOH and SAN copolymers were compared to investigate the effect of the polar interaction energy between the polymer and clay on the degree of intercalation. Although the initial penetration of the polymer occurred more effectively for EVOH because of its strong hydrophilic nature, the dissociation of clay platelets was better developed for SAN, proving that the glue effect is one of the key factors to govern the properties of polymer/clay nanocomposites.

The mechanical properties of the EVOH/clay nanocomposites were found to be superior to those of SAN/clay nanocomposites. Although dissociation of the respective clay layers was poorly produced for EVOH/clay nanocomposites, strong attractive energy

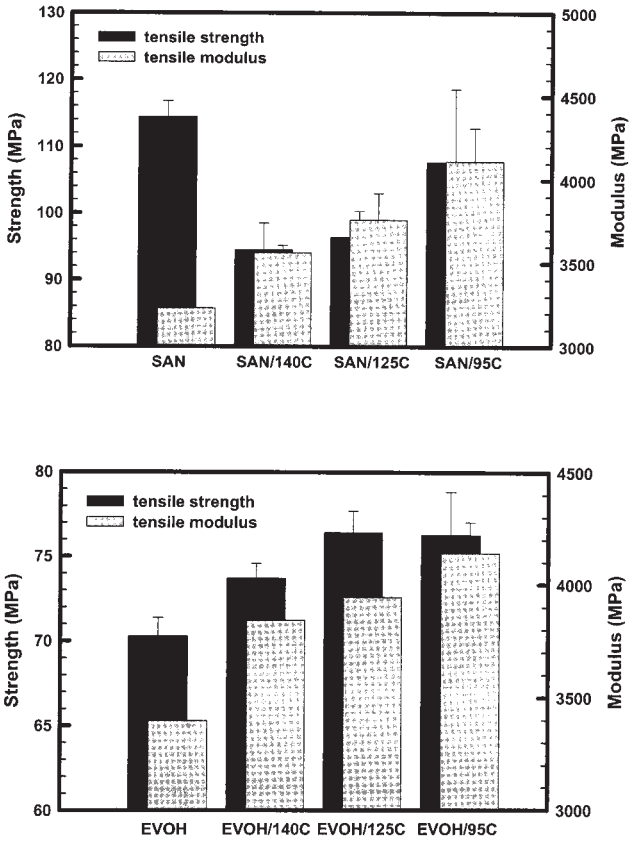


**Figure 3** The tensile properties of the intercalated SAN/clay and EVOH/clay nanocomposites prepared by dynamic melt intercalation. SAN/clay nanocomposites of intercalated structure exhibit lower tensile strength than neat SAN, and EVOH/clay nanocomposites show a noticeable increase of the tensile strength as well as modulus, implying enhanced adhesion at the interface.

very effectively stabilized the interface between the inorganic nanoparticles and the polymer matrix, resulting in higher mechanical properties.

This research was kindly supported by a grant from the Center for Advanced Materials Processing of the 21st Century Frontier R&D Program funded by the Ministry of Science and Technology, Korea, and an internal grant from the Korea Institute of Science and Technology. The XRD experiments were partly supported by the Ministry of Science and Technology, Korea, and the Pohang Acceleration Laboratory.

## References

1. Whitesides, G. M.; Mathias, T. P.; Seto, C. T. Science 1991, 254, 1312.
2. Gleiter, H. Adv Mater 1992, 4, 474.
3. Novak, B. Adv Mater 1993, 5, 422.
4. Burnside, S. D.; Giannelis, E. P. Chem Mater 1995, 7, 1597.
5. Giannelis, E. P. Chem Mater 1996, 8, 29.
6. Krishnamoorti, R.; Giannelis, E. P. Macromolecules 1997, 30, 4097.
7. Vaia, R. A.; Ishii, H.; Gianellis, E. P. Chem Mater 1993, 5, 1694.
8. Messersmith, P. B.; Giannelis, E. P. Chem Mater 1993, 5, 1064.
9. Okada, A.; Kawasumi, M.; Usuki, A.; Kojima, Y.; Kurauchi, T.; Kamigaito, O. Mater Res Soc Symp Proc 1990, 171, 45.
10. Okada, A.; Kawasumi, M.; Kurauchi, T.; Kamigaito, O. Polym Prepr 1987, 28, 447.
11. Fukushima, Y.; Okada, A.; Kawasumi, M.; Kurauchi, T.; Kamigaito, O. Clay Miner 1988, 23, 27.
12. Usuki, A.; Kawasumi, M.; Kojima, Y.; Okada, A.; Kurauchi, T.; Kamigaito, O. J Mater Res 1993, 8, 1174.
13. Lan, T.; Kaviratna, P. D.; Pinnavaia, T. Chem Mater 1995, 7, 2144.
14. Wang, M.; Pinnavaia, T. Chem Mater 1994, 6, 468.
15. Messersmith, P. B.; Giannelis, E. P. Chem Mater 1994, 6, 1719.
16. Akelah, A.; Moet, A. J Mater Sci 1996, 31, 3589.
17. Lyatskaya, Y.; Balazs, A. C. Macromolecules 1998, 31, 6676.
18. Balazs, A. C.; Singh, C.; Zhulina, E. Macromolecules 1998, 31, 8370.
19. Zhulina, E.; Singh, C.; Balazs, A. C. Langmuir 1999, 15, 3935.
20. Lee, S.-S.; Lee, C. S.; Kim, M.-H.; Kwak, S. Y.; Park, M.; Lim, S. H.; Choe, C. R.; Kim, J. J Polym Sci Part B: Polym Phys 2001, 39, 2430.
21. Lee, S.-S.; Kim, J. J Polym Sci Part B: Polym Phys 2004, 42, 246.
22. Lee, S.-S.; Kim, J. J Polym Sci Part B: Polym Phys 2004, 42, 2367.
23. Van Krevelen, D. W. Properties of Polymers, Their Estimation and Correlation with Chemical Structure, 2nd ed.; Elsevier: New York, 1980.